

Effect of Er³⁺ dopant on microstructure and photocatalytic property of nano-TiO₂

FAN Cai-mei(樊彩梅), TANG Qi(唐琦), WANG Yun-fang(王韵芳),
HAO Xiao-gang(郝晓刚), LIANG Zhen-hai(梁镇海), SUN Yan-ping(孙彦平)

College of Chemistry & Chemical Engineering, Taiyuan University of Technology, Taiyuan 030024, China

Received 15 July 2007; accepted 10 September 2007

Abstract: The nano-TiO₂ doped with Er³⁺ were prepared from Ti(OC₄H₉)₄ by sol-gel method, and the effect of Er³⁺ dopant on microstructure and photocatalytic activity of nano-TiO₂ was studied. The phase composition and crystallite sizes of Er³⁺-doped TiO₂ samples were analyzed by X-ray diffractometry (XRD) and transmission electron microscopy (TEM). The photocatalytic activity of Er³⁺-doped TiO₂ was investigated at different doping concentrations and different heat treatment temperatures in the photocatalytic degradation of phenol with 365 nm wavelength ultraviolet light irradiation. The results show that both the anatase phase and rutile phase are formed in doped TiO₂. Er³⁺ doping hinders the crystal transformation and makes the TiO₂ crystallite size change smaller as well as increases the photocatalytic activity of TiO₂ greatly. When Er³⁺ doping concentration is 1.2%(mass fraction) and the heat treatment temperature is 700 °C, the photocatalytic activity of Er³⁺-doped TiO₂ is favorite in the experimental range. The photocatalytic activity is enhanced by about 18% compared with that of the pure TiO₂ and almost approaches the photocatalytic activity of P₂₅-TiO₂.

Key words: photocatalysis; nano-TiO₂; Er³⁺ doping; phenol

1 Introduction

Photocatalytic technology using TiO₂ as catalyst has potential application in treatment of wastewater containing organics because it can degrade organic substance into CO₂, water and inorganic acid[1]. But the wide band gap of TiO₂(3.2 eV) and the invalid recombination of photo-hole and photo-electron produces a lower reaction rate in the photocatalytic process and inhibits the practice utilization of this technology. Thus, to improve the photocatalytic activity of TiO₂, doping other suitable ions into nano-TiO₂ is an effective way[2-5].

Rare earth element has f electron, easy to form various kinds of compounds, and its oxide also has crystalline structure, good stability, the function of influencing the conversion of crystal-phase state and changing the crystal grain size when it exists in other main oxide as dopant, therefore it has been used in lots of field[6-8]. Many results have revealed that doping rare earth ions into nano-TiO₂ can improve the

photocatalytic activity of TiO₂[9-11]. The previous study results about doping rare earth Y³⁺ and Ce³⁺ into TiO₂ demonstrated that suitable doping could make the absorption band of TiO₂ move toward the visible light region and increased the ability of absorbing light as well as improved the photocatalytic activity of TiO₂[12]. This work was designed to prepare Er³⁺/TiO₂ nano-powders by sol-gel method, and characterize their XRD, TEM patterns, then applied this doped TiO₂ in photocatalytic degradation of phenol in water and tried to give a clear relationship between Er³⁺/TiO₂ nano-powders and their photocatalytic activity.

2 Experimental

2.1 Reagents and apparatus

Anhydrous ethanol was purchased from Taiyuan Chemical Factory and Er(NO₃)₃·6H₂O was purchased from Ruiker Rare Earth Metallurgy and Functional Material State Engineering Research Institution. Phenol chemical was in analytic grade and was purchased from Beijing Chemical Plant. Ti(OC₄H₉)₄ was purchased from

Tianjin Chemical Reagent Factory. All the other reagents were in analytic grade.

2.2 Preparation of catalyst

Water, $\text{Ti}(\text{OC}_4\text{H}_9)_4$ and anhydrous ethanol were mixed in terms of mass ratio of 1:3:12. First $\text{Ti}(\text{Obu})_4$ were dissolved in $\text{Er}(\text{NO}_3)_3 \cdot 6\text{H}_2\text{O}$ anhydrous ethanol solution, then nitric acid was used to adjust the pH value of solution to 2 and the distilled water was added into the solution. The solution was vigorously stirred for 1 h in order to form sols. After aging for 5 h, the sols transformed into gels. The gels was dried under 100°C in order to evaporate water and organic material as much as possible. Then the dry gels were ground in a ball mill and calcined at certain temperature in oven. By this procedure the dopant Er^{3+} nano- TiO_2 powders were obtained.

2.3 Characterization of photocatalysts

In order to determine the crystal phase composition of the doped photocatalyst powders, X-ray powder diffraction(XRD) patterns were recorded at $2\theta=10^\circ\text{--}80^\circ$ on a Rigaku D/max2500 with Cu K radiation using the Debye-Scherrer technique. Transmission electron microscopy(TEM) was carried out on JEM-200FX II.

2.4 Photocatalytic activity experiments

The activity experiments of photocatalysts were performed in a batch slurry cylindrical quartz photoreactor with effective reactive volume of 50 mL. The photodegraded solution was phenol solution (20 mL/L) prepared with distilled water and analytic grade phenol. The slurry suspension for photocatalytic reactions was prepared by adding 1 g/L TiO_2 or doping TiO_2 nano-powders into phenol solution through stirring. Before the light is turned on, the solution was stirred for 30 min to ensure a good adsorption equilibrium between the catalyst and the solution. During the photocatalytic reaction, the solution was aerated by bubbling air and irradiated using a 250 W UV light($\lambda=365\text{ nm}$) positioned by the reactor. At different irradiation time intervals, the samples of phenol solution were drawn and analyzed to determine the concentration of phenol and TOC(total organic carbon). The concentration of phenol in the solution was analyzed by UV-VIS spectrophotometer (Shanghai Third Analytic Instrument Plant) at 510 nm by 4-amionantipyrin method. TOC concentration in water samples was measured by TOC instrument Multi N/C 3 000 (Germany Yena Company) with results expressed in mg/L.

3 Results and discussion

3.1 XRD patterns and TEM images of Er^{3+} doped TiO_2

3.1.1 Phase structure of TiO_2 doped with Er^{3+}

Fig.1 shows XRD patterns of doped TiO_2 powder calcined at 700°C with different Er^{3+} contents(mass fraction) of 0, 0.8%, 1.2%, 1.5% (Fig.1(a) shows anatase phase diffraction apex and Fig.1(b) shows rutile phase diffraction apex). These patterns show that the TiO_2 compound nano-powders are mixture of rutile and anatase phase. Compared with pure TiO_2 nano-powders, the apexes of doped nano-powders have a little movement, which indicates that the doping may leads to the change of crystal lattice parameters.

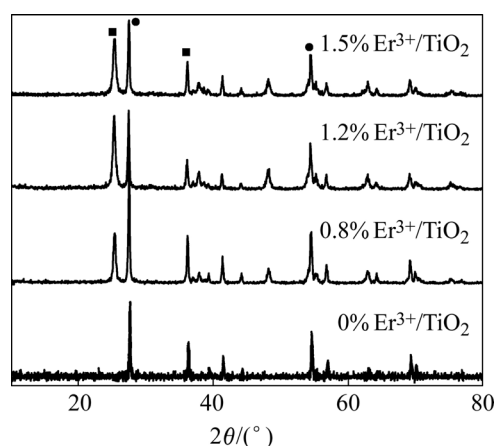


Fig.1 XRD patterns of $\text{Er}^{3+}/\text{TiO}_2$ powders

Using the quantitative equation: $X_A=1/(1+1.26I_A/I_B)$, where I_A and I_B are X-ray integrated intensities of $2\theta=25.3^\circ$ reflection of anatase and $2\theta=27.4^\circ$ reflection of rutile, respectively. The content of anatase in calcined TiO_2 at 700°C with different doping levels can be calculated. The results are given in Table 1. Table 1 displays that the mass fractions of anatase and rutile in pure TiO_2 are different from those of doped TiO_2 . The doping restrains the conversion of anatase to rutile in some extent.

Table 1 Effect of Er^{3+} contents on anatase contents of TiO_2

$w(\text{Er}^{3+})/\%$	0	0.8	1.2	1.5
$w(\text{Anatase of TiO}_2)/\%$	2.7	38.57	48.16	44.50

Using the Scherrer estimation: $D=K\lambda/(\beta\cos\theta)$, the average anatase grain size of TiO_2 powders was determined by the broadening of the anatase peak ($2\theta=25.3^\circ$). The results are given in Table 2. In comparison with the pure TiO_2 samples, the doped ones have relatively small particle size, indicating that the doping can improve the particle morphology, and retard the grain growth of TiO_2 . The reason may be that some Ti^{4+} atoms in crystal lattice are replaced by Er^{3+} during the heat-treatment process, leading to the local lattice distortion, which prevents the movement of crystal interphase and the growth of TiO_2 crystal grain[13–14].

Table 2 Effect of Er^{3+} contents on particle sizes of $\text{Er}^{3+}/\text{TiO}_2$

$w(\text{Er}^{3+})/\%$	0	0.8	1.2	1.5
Particles size/nm	172.39	52.70	38.03	68.32

3.1.2 TEM micrographs of pure TiO_2 and doped TiO_2 with $w(\text{Er}^{3+})=1.2\%$

Fig.2 shows TEM micrographs of pure TiO_2 and doped TiO_2 with $w(\text{Er}^{3+})=1.2\%$ calcined at $700\text{ }^\circ\text{C}$. The results show that doping can retard the development of grain size of TiO_2 and decrease the diameter of TiO_2 . The mean diameter of $\text{Er}^{3+}/\text{TiO}_2$ is about $40\text{--}70\text{ nm}$, which is smaller than that of pure TiO_2 . This is correlated with the calculation results with Scherrer estimation.

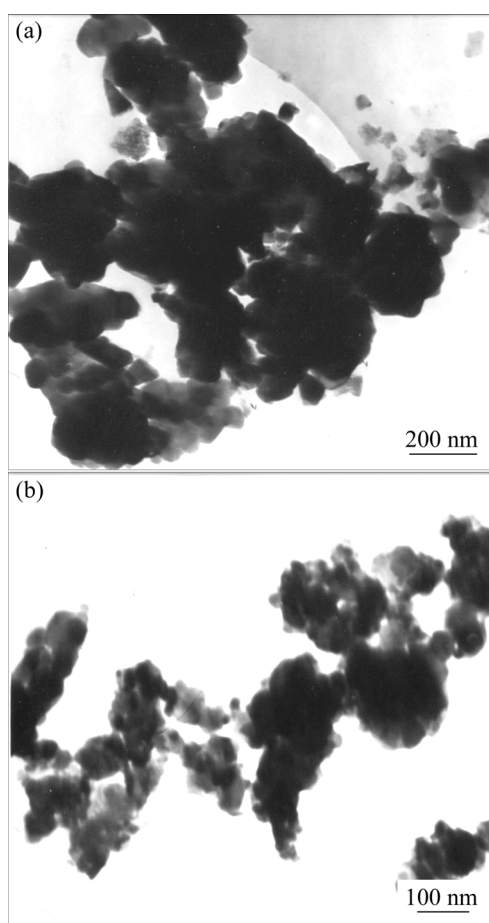


Fig.2 TEM micrographs of TiO_2 nano-powder: (a) Pure TiO_2 ; (b) $\text{Er}^{3+}/\text{TiO}_2$

3.2 Photocatalytic activity of doped TiO_2

3.2.1 Effect of doped concentration of Er^{3+} on photocatalytic activity

In order to study the effect of different Er^{3+} doped concentrations on the photocatalytic activity of TiO_2 , four phenol degradation experimental processes were conducted under $10.5\text{ mW}/\text{cm}^2$ light intensity irradiation with different Er^{3+} concentrations of 0, 0.8%, 1.2% and 1.5%, and the results are shown in Fig.3.

The experimental results indicate that the phenol

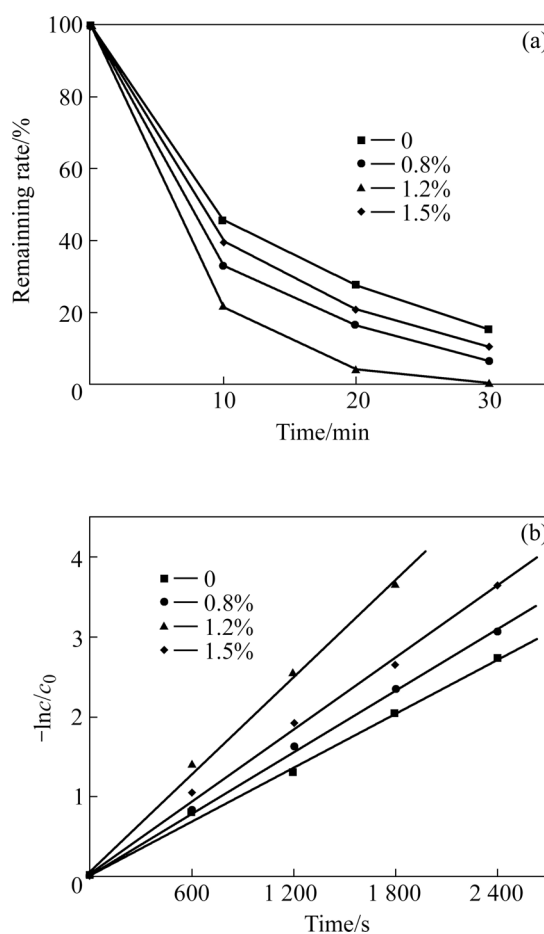


Fig.3 Effect of Er^{3+} doping concentrations on photocatalytic activities of TiO_2 : (a) Remaining rate of phenol; (b) $-\ln c/c_0$ vs time

remaining rates in solution are 15%, 6.3%, 0, 10.6%, respectively, for different Er^{3+} concentration of 0%, 0.8%, 1.2% and 1.5%, which demonstrates that there exists an optimal Er^{3+} concentration for the photocatalytic activity of TiO_2 in degradation of phenol, when the content of Er^{3+} is among 0–1.2%. Doping can significantly improve the photocatalytic activity of TiO_2 , but when the dopant concentration is more than 1.2%, the photocatalytic activity decreases, which means that more doping can convert the dopant from the trap center to the combination center of electron and hole[15] and makes the photocatalytic ability of TiO_2 decrease. On the other hand the band gap of semiconductor changes wider with the crystal grain decrease in the nano-dimension, then the photo-electron and photo-hole possess stronger oxidation and reduction[16]. In this study, due to the doping of Er^{3+} in TiO_2 , the grain size and the anatase phase are changed, which is also favorable for the increase of photoactivity. Compared with pure TiO_2 , the doped TiO_2 with 1.2% Er^{3+} makes the degradation rate of phenol enhanced by about 18%.

As shown in Fig.3(b), the relationship between $-\ln c/c_0$ and irradiation time is linear, which means that the degradation of phenol follows pseudo first-order kinetics. Generally speaking, the larger the slope of pseudo first-order linear equation, the stronger the photoactivity of the photocatalyst[17]. The results in Fig.3(b) further demonstrates that 1.2% Er^{3+} dopant is suitable for the photocatalytic application of TiO_2 , therefore in the following experiments, this doped TiO_2 was used as photocatalyst.

3.2.2 Effect of heat treatment temperature on photocatalytic activity

Fig.4(a) shows the degradation of phenol in solution using Er^{3+} doped TiO_2 photocatalysts calcinated at different temperatures of 500, 600, 700 and 800 °C. The photocatalyst calcinated at 700 °C expresses a better photoactivity. The phenol in solution is removed completely after 30 min reaction. TOC concentration obtained at contained time reveals analogous trends, as seen in Fig.4(b). These results clearly demonstrate that the degradation rate increases with the increase of heat treatment temperature of $\text{Er}^{3+}/\text{TiO}_2$ up to 700 °C,

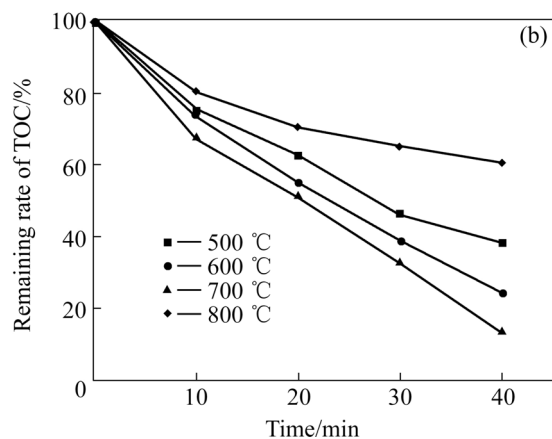
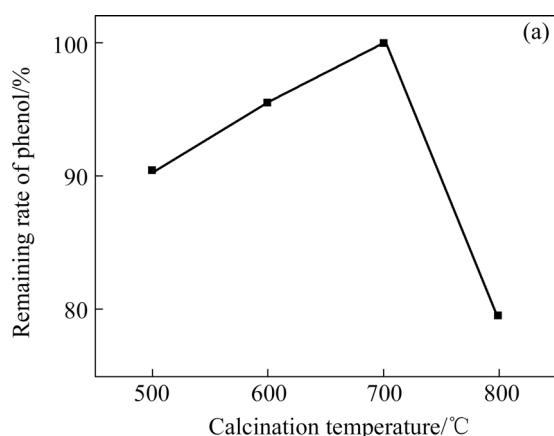


Fig.4 Effect of different calcination temperatures on photocatalytic activity of $\text{Er}^{3+}/\text{TiO}_2$: (a) Remaining rate of phenol; (b) Remaining rate of TOC

and further increasing heat treatment temperature leads to a obvious decrease in degradation. This feature indicates that the heat treatment temperature has an important influence on photoactivity of TiO_2 .

3.2.3 Comparison of photoactivity between $\text{Er}^{3+}/\text{TiO}_2$ and $\text{P}_{25}\text{-TiO}_2$

In this study a degradation test was designed for comparing the photoactivity of pure $\text{P}_{25}\text{-TiO}_2$ (Germany Degussa) with nano- $\text{Er}^{3+}/\text{TiO}_2$ lab-made under the favorite experimental conditions of Er^{3+} concentration of 1.2%, $\text{Er}^{3+}/\text{TiO}_2$ calcinated temperature of 700 °C and the light intensity of 10.5 mW/cm^2 . The results of phenol remaining rate are shown in Fig.5. From Fig.5 it can be seen that the phenol in solution is degraded completely in both reaction processes after 30 min reaction, but the $\text{P}_{25}\text{-TiO}_2$ photoactivity is still higher than that of $\text{Er}^{3+}/\text{TiO}_2$. The degradation rate of the former is 96.1% and the latter is 78.6% after reaction lasts for 10 min. This different photoactivity maybe attributes to the different preparation method.

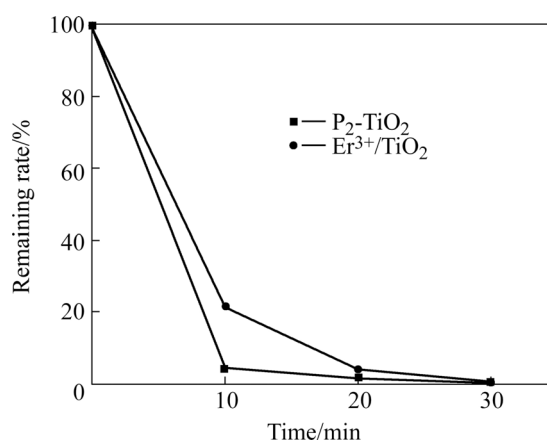


Fig.5 Comparison of photocatalytic activities of $\text{Er}^{3+}/\text{TiO}_2$ and $\text{P}_{25}\text{-TiO}_2$

4 Conclusions

1) Nano- TiO_2 doped with Er^{3+} is prepared by gel-sol method. Compared with pure TiO_2 , Er^{3+} doping hinders the crystal transformation and makes the TiO_2 crystallite size change smaller as well as increases the photocatalytic activity of TiO_2 greatly.

2) The Er^{3+} doping concentration of 1.2%(mass fraction) is favorite for the photocatalytic degradation, and the grain diameter of doped nano- TiO_2 is the smallest in experimental range. The photocatalytic activity is enhanced by about 18% compared with that of the pure TiO_2 .

3) Heat treatment temperature has effect on the crystal state and grain diameter, and has further effect on the photocatalytic activity. When the heat treatment temperature is 700 °C, the doped nano- TiO_2 expresses a

higher photoactivity in the degradation process of phenol.

4) The comparison experiments of photoactivity between $\text{Er}^{3+}/\text{TiO}_2$ and $\text{P}_{25}\text{-TiO}_2$ show that the degradation velocity of $\text{P}_{25}\text{-TiO}_2$ are faster than that of the lab-made $\text{Er}^{3+}/\text{TiO}_2$, but the difference is very little.

References

- [1] HOFFMANN M R, MARTIN S T, CHOI W Y, et al. Environmental application of semiconductor photocatalysis[J]. *Chem Rev*, 1995, 95: 69–96.
- [2] XU A W, GAO Y, LIU H Q. The preparation, characterization and their photocatalytic activities of rare-earth-doped TiO_2 nano particles[J]. *J Cataly*, 2002, 207(2): 151–157.
- [3] BUTLER E C, DAVIS A P. Photocatalytic oxidation in aqueous titanium dioxide suspensions: The influence of dissolved transition metals[J]. *Photo Chem Photochem Photobiol A: Chem*, 1993, 70: 273–283.
- [4] SERPONE N, DISIDIER J. Spectroscopic, photoconductivity, and photo-catalytic studies of TiO_2 colloids: Naked and with the lattice doped with Cr^{3+} , Fe^{3+} , and V^{5+} cations[J]. *Langumir*, 1994, 10(3): 643–652.
- [5] LITTER M I, NAVIO J A. Photocatalytic properties of iron-doped titania semiconductors[J]. *J Photochem Photobiol A: Chem*, 1996, 98: 171–181.
- [6] LI Hong-yu, YU Gui, LIU Yun-qi, et al. Luminescent materials with sharp spectral bands and electroluminescent device[J]. *Rare Earth*, 2000, 21(4): 61–64.(in Chinese)
- [7] FRINDELL K L, BARTL M H, ROBINSON M R, et al. Visible and near-IR luminescence via energy transfer in rare earth doped mesoporous titania thin films with nanocrystalline walls[J]. *Journal of Solid State Chemistry*, 2003, 172(1): 81–85.
- [8] LETTMANN C, HILDENBRAND K, KISCH H, et al. Visible light photocatalytic degradation of 4-chlorophenol with a coke-containing titanium dioxide photocatalyst[J]. *Applied Catalysis B: Environmental*, 2001, 32 (4): 215.
- [9] YU J C, LIN J, KWOK W M. Enhanced photocatalytic activity of $\text{Ti}_{1-x}\text{V}_x\text{O}_2$ solid solution on the degradation of acetone[J]. *J Photochem Photobiol A*: 1997, 111: 199–203.
- [10] XU Bei-xue, WU Jin-lei. Effects of neodymium on the size of silver nano-particles prepared by vacuum deposition[J]. *Rare Metal Materials and Engineering*, 2003, 32(10): 818–821.(in Chinese)
- [11] GAO Yuan, XU An-wu, ZHU Jing-yan, et al. Study on photocatalytic oxidation of nitrite over RE/TiO_2 photocatalysts[J]. *Chinese Journal of Catalysis*, 2001, 22(1): 53–58.(in Chinese)
- [12] FAN Cai-mei, XUE Peng, DING Guang-yue, et al. The preparation of nanoparticle Y^{3+} -doped TiO_2 and its photocatalytic activity[J]. *Rare Metal Materials and Engineering*, 2005, 34(7): 1094–1097.(in Chinese)
- [13] HOFFMANN A J, MILLS G, YEE H, et al. Photoinitiated polymerization of methyl methacrylate using Q-sized zinc oxide colloids[J]. *J Phys Chem*, 1992, 96: 5540–5545.
- [14] HOFFMANN A J, YEE H, MILLS G, et al. Q-sized cadmium sulfide: Synthesis, characterization, and efficiency of photoinitiation of polymerization of several vinylic monomers[J]. *J Phys Chem*, 1992, 96: 5546–5552.
- [15] HIDAKA H, KAZUKIKO T S, ZHAO J, et al. Photoelectrochemical decomposition of amino acids on a TiO_2/OTE particulate film electrode[J]. *J Photochem Photobiol*, 1997, 109: 165–170.
- [16] BRUS L E. Electronic wave functions in semiconductor clusters: experiment and theory [J]. *J Phys Chem*, 1990, 90: 2555–2560.
- [17] LI Fang-bai, GU Guo-bang, LI Xin-jun, et al. Preparation, characterization and photo-catalytic behavior of $\text{Y}_2\text{O}_3/\text{TiO}_2$ composite semiconductor nanopowder[J]. *Journal of the Chinese Rare Earth Society*, 2001, 19(3): 225–228.(in Chinese)

(Edited by CHEN Can-hua)